Reviews on dimer model

Le rapport de stage du M1 DMA,

École Normale Supérieure de Paris

Tiancheng He,
under the supervision of Prof. **Dmitry Chelkak**

September 7, 2021

summery

In this report, we briefly review the theories of the dimer model in the past 20 years.

In the introduction chapter, we give the definitions of the model and then introduce the 3 most important problems concerned in this field: the limit shape, the fluctuations, and the local limit.

In chapter 2, we answer the limit shape problem, based on the famous paper [3].

In chapter 3, we investigate the local limit mainly based on [8]. We firstly introduce the classical Kasteleyn Matrix theory, and then use it to distinguish the "3 phases" in the local limit.

Finally, in chapter 4, we go to the fluctuations. We review the Kenyon-Okounkov conjecture, which remains the most important open problem in this field. In this chapter, we firstly provide a heuristic to the conjecture, then introduce the 2 different approaches to the conjecture.

This report aims to let those who do not work in this field understand the recent progress, hence we will not go through formal definitions and proofs but focus on the intuitions and ideas in developing these theories. For formal theorem and proofs, I strongly recommend you to read the references.

Acknowledgments

Firstly, the training is under the supervision of professor Dmitry Chelkak, and I'm grateful for his numerous instructions and discussions in 3 months. Also, I want to thank Yijun Wan for her discussion and useful advice for this report.

Moreover, thanks to professor Xinyi Li for inviting me to give a 4 hours' lecture in Peking University based on this training, and also to the audiences who provided many interesting viewpoints and questions.

Contents

Chapter 1

Introduction

This chapter is mainly based on [5] and the introduction chapter of all other references.

Dimer model has been an important model in physics. Various fields have been involved in studying dimer models, including analysis, probability, representation theory, etc. For the Dimer model, the general setup is to take a *lattice domain* and tiles it with *elementary block*. Here are 2 basic examples:

Definition 1.1. A *lozenge tiling* is a way of covering a triangle grid by 3 kinds of 60-degree rhombis (called lozenges) so that there are no gaps or overlaps.

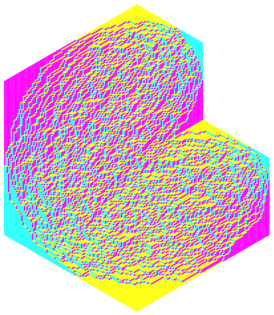

Figure 1.1: Illustrations a typical lozenge tiling, where different color represent for different type of dimer, [5].

Definition 1.2. A *domino tiling* is a way of covering that region with dominos(1×2 or 2×1 rectangles) so that there are no gaps or overlaps.

Equivalently, we can choose the dual graph of the domain, and a dimer configuration is a perfect matching[1] in the dual graph. Fixed such a domain (or equivalently the dual graph), we put a uniform distribution on all dimer configurations, then get a probability model, which is called the *dimer model*.

Remark 1.1. *Sometimes we consider the weighted model, i.e. for each edges in the dual graph, we put a weight $w(e)$ on it. Then a dimer configuration with edges $e_1, \ldots, e_n$ appears with probability $\prod_{i=1}^{n} w(e_i)/Z$, where the* partition function $Z = \sum_{matching} \prod_{i=1}^{n} w(e_i)/Z$

[1] a subgraph that all vertices have degree 1

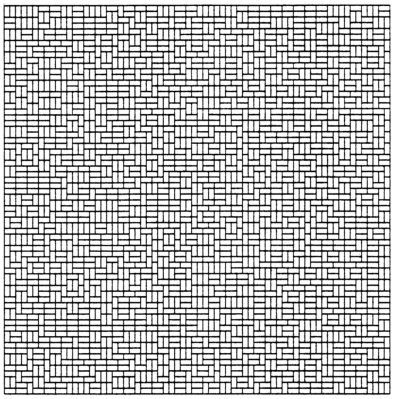

FIGURE 1. A random domino tiling of a square.

Figure 1.2: A typical domino tiling, [8].

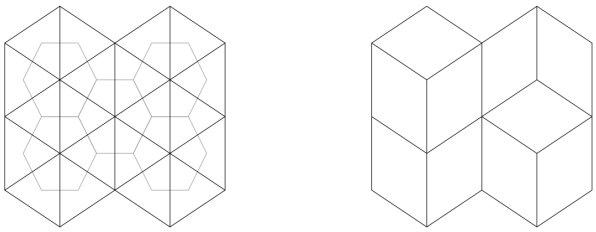

Figure 1.3: Illustrations of a graph and dual graph [4]

Generally speaking, we want to understand the *typical behavior* of the configurations for a very large domain, or equivalently, when mesh sizes (of the elementary block) are small.

We introduce the *height function* which is the main object we investigate. The height function can be defined on all models, but here we will first define lozenge tilings and domino tilings.

Definition 1.3 (height function on lozenge tiling)**.** Given a dimer configuration of lozenge tiling, we define the height function as follow: for 2 adjacent point u, v and (uv) not cross a lozenge, let let $h(v) - h(u)$=1 when (u, v) has positive direction(in the picture); and negative elsewhere.

We can check that the height change around a lozenge is 0 so that it's well defined on all vertex up to a global shift.

Remark 1.2. *The height function on lozenge tiling has a good intuition: we can view the lozenge tiling as orthogonal projections of a 2d surface onto the $x + y + z = 0$ plane of three sides of a unit cube, and the height function is the original surface height.*

Remark 1.3. *We can see that as $h(v)$ fixed for one v, the residue module 3 of a vertex is determined. Hence height function has another interpolation: a function with the right residue at each point, and with height change $\pm 1, \pm 2$ at each adjacent pair. (only ± 1 at the boundary)*

Definition 1.4 (height function on domino tilings)**.** For domino tilings, we don't have such a good 3d view, while the definition is similar. As remark before, we firstly fixed the residue of 4

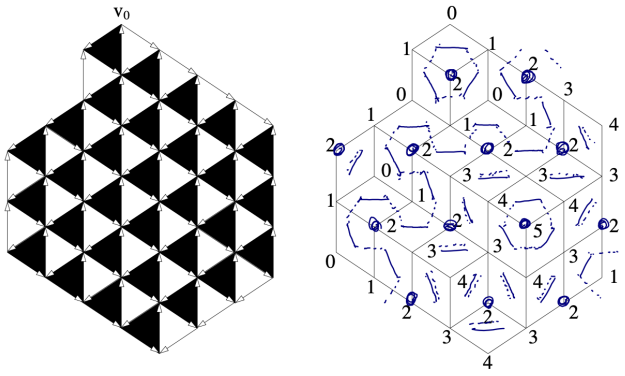

Figure 1.4: Illustrations of the height function in a lozenge tiling [4]

at each vertex(embed the lattice in $\mathbb{Z}^2$, and let point at (x, y) with residue $(x+y) \pmod 4$), and then let the height change at an edge be $1, -1$ if it doesn't cross a domino, and $3, -3$ otherwise.

As a direct consequence, we notice that the boundary(outer cycle) height function can be defined (up to a constant shift) independent of the dimer inside(if there exists a dimer configuration). Also, the behavior of the boundary height function is irrelevant to the shape of the domain. For example, a *Temperley domain* always has a flat boundary condition(the boundary height difference is within constant), while the shape could be anything.

As height function is equivalent to a dimer configuration, so that understanding the typical behavior of dimer is equivalent to understand the height function behavior. We can prove that the typical behavior of the height function only relies on the limit domain shape and the "limit boundary condition"(The limit asymptotic of the height function on the boundary). Look at *domino tiling on Temperley domain*, *Aztec diamond* or *Lozenge tiling on large hexagon* as classical example.

Specifically, we are interested in the following questions :

1. **The Law of large numbers.** Each lozenge tilings is a projection of a 2d–surface and therefore can be represented as a graph of a function of two variables which we call the *height function*. If we take a uniformly random tiling of a given domain, then we obtain a random height function $h(x, y)$ encoding a random stepped surface. What is happening with the random height function of a domain when the mesh sides turn to 0?

[3] proved the law of large numbers that the rescaled height function has a deterministic limit. i.e. there's a *limit shape* $\hat{h}$ such that:

$$\lim_{L\to\infty} \frac{1}{L} h(Lx, Ly) = \hat{h}(x, y) \tag{1.1}$$

The limit shape is a deterministic function(a maximizer of the *entropy function*) given the boundary condition. We will invest this problem in section 2.

2. **Analogs of the Central Limit Theorem.** The next goal is to understand the fluctuations of the height function around the asymptotic limit shape, i.e. to identify the limit

$$(h(nx, ny) - E[h(nx, ny)]) \to GFF \tag{1.2}$$

Note that here we don't need to divide h by n as in the classical CLT; because the fluctuations are much smaller. $\xi(x, y)$ denotes the limiting random field, in this case, it can be identified with the (modified) *Gaussian free field*. The GFF is related to conformal geometry as it turns out to be invariant under conformal transformations. We will invest this problem in sections 4 and 5.

3. **Local limit and "phase transition".** Observe the typical lozenge tiling, it's almost flat at the corner of the hexagon and fluctuated in the bulk. We call the former *frozen region*, and the latter *liquid region*, and there's an arctic curve that separates these regions, so in the limit shape there's a "phase transition". In fact, in a general situation, if we properly choose the weight $w(e)$, there should be another kind of situation called the "gaseous phase".

In different phrases, the height correlation behavior is different. We can distinguish these situations by *slopes*.

we will invest this problem in section 3.

Remark 1.4. *Given a domain, is there exist a tiling in the domain? Of course, we need the vertices in the dual graph to be even; and if the dual graph is bipartite, we also need the vertices in each part to be the same. But this is still not sufficient. However, fortunately, we have a simple answer based on the height function: if the height function is well defined on the boundary, and it satisfies $h(u) - h(v) \leq d(u, v)$ for all boundary point u, v, then the domain is tillable. ([5] 1.4)*

Chapter 2

The limit shape

This section is mainly based on the famous paper [3]. The main theorem is Theorem 2.2, where we prove that the height function h converges to a given limit shape in probability. Now, let us start with a theorem that counts the (exp-order of) number of configurations near a given height function.

Theorem 2.1 ([3] Thm 4.3)**.** *For regular region R^* [1] and good asymptotic height function h [2], and let good region R approximates R^* when it normalized by $1/n$.*

Then the number of tilings of R whose normalized height functions are within $O(\delta)$ of h is

$$\exp\left(n^2 area(R^*)(Ent(h) + o(1))\right),$$

as $\delta \to 0$ (for n sufficiently large).

Remark 2.1. *The 2-Lipschitz comes from the combinatorics fact that if u and v are lattice points at sup norm distance at most d from each other within R, we can check that $|h(u)-h(v)| \leq 2d+1$. for any height function h.*

Let the tilt *of f be $(s,t) = (\frac{\partial f}{\partial x}, \frac{\partial f}{\partial y})$, then we have an asymptotic height function f should satisfy $|s| + |t| \leq 2$ at any point.*

Remark 2.2. *The entropy function is defined as*

$$Ent(h) = \frac{1}{area(R)} \iint_{R^*} ent\left(\frac{\partial h}{\partial x}, \frac{\partial h}{\partial y}\right) dxdy$$

where $ent(s,t) = 1/\pi \cdot (L(\pi p_a) + L(\pi p_b) + L(\pi p_c) + L(\pi p_d))$,

$L(x) = -\int_0^z \log|2\sin t|dt$

and $p_a = s/4 + 1/2\pi \arccos(\cos(\pi s/2) - \cos(\pi t/s)/2)$ (p_b, p_c, p_d is defined similar in [3](1.8))

Here the "entropy" refers to entropy per domino, i.e. the normal entropy(equals $\log$(number of configurations)) normalized by dividing by the number of dominos in a tiling of R.

We can prove that it is upper semi-continuous.

From this theorem, we can derive without much difficulty that the limit shape converges to the maximizer of the entropy:

[1] bounded by a simple closed curve

[2] 2-Lip with boundary condition h_b

Theorem 2.2 ([3] Thm 1.1)**.** *Let R^* be a good region* [3]*, and h_b be a good* [4] *asymptotic boundary height function.*

Suppose that $h^* : R^* \to \mathbb{R}$ is the unique *such Lipschitz function maximizing the entropy functional $Ent(h^*)$, subject to $h^*|\partial R^* = h_b$;*

Let R be a lattice region that approximates R^* when rescaled by a factor of $1/n$, and whose normalized boundary height function approximates h_b. Then the normalized height function of a random tiling of R approximates h^* (with probability tending to 1 as $n \to \infty$).

Proof by Thm 2.1. As the 2-Lipschitz family is relatively compact, (Arzela-Ascoli Lemma), we can cover the function space by ϵ-balls. Notice that in a ϵ-ball does not contain the unique f, the number of tilings is n^2-exponentially small (compare to the one that contains f), hence with large probability, they are concentrated in the ϵ-ball of f. □

Remark 2.3. *The "near" is define as follows:*

the logarithm of the number of tilings of R whose normalized height functions are within $O(\delta)$ of h is the area of R times $Ent(h) + o(1)$ as $\delta \to 0$ (for n sufficiently large).

Define a free tiling (or a "tiling with free boundary conditions") of a region as a covering of the region by dominos, no two of which overlap, and each of which contains at least one cell belonging to the region. Free tiling is just like normal tiling, except that the tiles are allowed to cross the boundary.

Next, we focus on Theorem 1, i.e. counting the number of tiling near a given height h.

The key lemma is the following, which proves that the number asymptotic is continuous about the boundary condition(when it's near a plane).

Lemma 2.1 ([3] Prop 3.6)**.** *Consider a good region*[5] *R located in a $n \times n$ square. For $\epsilon > 0$, suppose that h is a boundary height function on R that is fit to within $\epsilon A/n$ by a fixed plane(linear).*

Then the entropy of extensions of h to R is independent of the precise boundary conditions, up to an error of $O(\epsilon^{1/2} \log 1/\epsilon)$. (for A sufficiently large and ϵ sufficiently small)

scratch of the proof. When the tilt of the plane is large, i.e. $|s| + |t| \geq 2 - \epsilon^{1/2}$, we can directly calculate that the number of tiling is $O(\epsilon^{1/2} \log 1/\epsilon)$ in any boundary condition and we proved. ([3] prop 3.5)

Otherwise, for different boundary f and g, we can find a bijection coupling on the extension of f and g except for $O(\epsilon^{1/2} \log 1/\epsilon)A$ points, with high probability. Given the height function in these points, the possible extension for the points left is of order $\exp O(\epsilon^{1/2} \log 1/\epsilon)A$. We proved the lemma. □

Remark 2.4. *Basically, the coupling proof is like the 2d version of coupling of the random walk: we observe that for closed boundary conditions, the height function distribution at the edge is different, but in the bulk they are close. Hence we can define a couple at the time they meet, and then prove that they are meeting fast.*

Then, we have a classical calculations we can calculate the entropy in a torus with given "slope" (s, t) is $ent(s, t)$(the local entropy), and notice that the boundary condition doesn't matter, we get the entropy of an extension h with near planar boundary is $ent(s, t) + O(\epsilon^{1/2} \log 1/\epsilon)$ (thm 4.1).

For these calculations, we will go to the next section for detail.

[3] in $\mathbb{R}^2$ bounded by a piecewise smooth, simple closed curve ∂R

[4] $\partial R \to \mathbb{R}$ which can be extended to a function on R with Lipschitz constant at most 2 in the sup norm

[5] Fix $k > 0$, R is horizontally and vertically convex of area A, with at most n rows and columns, such that $kn^2 \leq A$ and $n \leq \epsilon A$.

Now we go back to the original problem. We understand well the entropy near a square. With some standard arguments, we can extend the conclusion to an equilateral triangle with a planar boundary. But how to extend to an arbitrary boundary? The method is a standard in analysis, that is cutting the region into small triangle pieces, and proof that the cutting "waste" is neglectable.

scratch of the proof of Thm 1. we can cut the region R^* into small triangles, such that at each triangle, the asymptotic height h and its derivative are regular(actually we can only be done this at a large proportion, but doesn't change the proof).

Cut the region R as in R^*, but let the boundary condition be near the local tilt of h. Then we consider the boundary of these "triangles", and call these boundaries *skeleton*).

The lower bound: we only consider the dimers that *not cross the skeleton*. then given the height function on the skeleton, the number tilings in a small triangle is $ent(s,t)$. Multiply them together and consider the logarithm we get whole entropy is the integral form $Ent(h)$.

The upper bound needs a trick: for the dimers crossing the skeleton, choose the inner boundary of the dimer. Then the number of such boundaries is of order $\exp o(n^2)$. Again, for each boundary, inside the triangle we get entropy $ent(s,t)$; and at the boundary (those dominos that cross the boundary) we have another $\exp o(n^2)$.

In all we get the entropy is $Ent(h)$.

□

Remark 2.5. *As the limit shape h is the function maximize $\iint_{R^*} ent(h_x, h_y)dxdy$, we can determine h as a solution of the Euler-Lagrange equations. (In liquid region)*

Chapter 3

Calculations and 3 phases

In this section, we introduce the classical result of calculating the partition function via the Kasteleyn matrix, following the method in [8].

3.1 Kasteleyn matrix, partition function on planar graph

How to calculate the number of tilings in a given domain? The questions have been answered by Kasteleyn in the 1970s. The number of tilings is the number of a perfect matching in the dual graph. We want to explain this by the determinant of a matrix so that we can calculate it by various methods.

Consider the dual graph of the domain, and suppose that it is bipartite(if it's not, then finally need to write the number in the Phaffian), and can be colored by white and black vertices. Now, consider the (modified) adjacent matrix of this bipartite graph: $M = (M(b, w))$(labeled by a black vertex b and white vertex w), where $m(b, w) = 1$ when there's an edge between b, w and $M(b, w) = 0$ otherwise. Then the number of tilings equals the permanents (determinant without the sign). To change the permanents to determinants, we can add a proper sign to each edge (or a complex number at the unit circle) to make all the perfect matchings have the same sign. That's the definition of the Kasteleyn matrix.

Definition 3.1 (Kasteleyn matrix)**.** The Kasteleyn matrix is defines as $K = (K(b, w))$, with $K(b, w) = 0$ if b, w not adjacent, and $|K(b, w)| = W(bw)$(edge weight).

Moreover, for each face $w_1, b_1, \ldots, w_d, b_d$(where $w_{d+1} = w_1$), it satisfies

$$X_f := (-1)^{d+1} \frac{\prod K(b_i, w_i)}{\prod K(b_i, w_{i+1})}$$

is a positive real.

And we can prove that in a Kasteleyn matrix the sign for all matching is the same, yield the following theorem:

Theorem 3.1. *The partition function equals*

$$Z = |\det K|$$

Proof. Any 2 configurations are different by some circles in the dual graph, which are correspond to some faces. Hence we only need to prove that two configurations that differ by a single face have the same sign. And after the calculation, this is just equivalent to $X_f = 1$. □

Remark 3.1. *When the graph is not bipartite, we need to consider the matrix $\tilde{K}(v,w)$ for all vertices v,w(which is twice the size of the matrix K), and to make the partition function equals the Phaffian of $\tilde{K}$.*

We can always find such matrix K a for a planar graph, by left a dual-tree uncertain and determine the sign(+1 or -1) one by one from the leaves of the tree. However, we hope that the weight we choose is periodic (at least regular) so that we can make a globally calculation. If we consider the weighted dimer model, we only need to multiply the weight in $K(b,w)$, and the theorem also holds.

Example 3.1. *In the dual graph of the lozenge tilings, all faces have 6 vertices, so we can just choose weight $K=1$ on each edge.*

Example 3.2. *For the square grid, we hope that the product of K at each face is -1, so we can just choose weights $1,i,-1,-i$ around each faces, and such that the graph is periodic.*

3.2 Partition function on torus

An important object we are interested in is the weighted double periodic graph(periodic in 2 directions) on a torus. In this subsection, we consider a $\mathbb{Z}^2$ periodic planar graph G, where the translation is color-preserving; and let G_n be the quotient of G by the action of $n\mathbb{Z}^2$.

Now we aim to give an asymptotic for the scaled partition function of G_n (or the free energy). A priori, we wish to use the same method as the planar case to choose the sign in the Kasteleyn matrix. Unfortunately, this is not possible, as here we not only consider the sign around a face but also around horizontal and vertical cycles. However, we can consider the summation of several determinants, and choose the sign properly so that the total weight for all configurations is the same. Specifically, we have (this is a classical result):

Theorem 3.2 ([8]3.1.2)**.** *The actual partition function can then be obtained as a sum of four determinants*

$$Z=(-Z^{(00)}+Z^{(10)}+Z^{(01)}+Z^{(11)})/2$$

where $Z^{(ij)}$ is the determinant of K in which the signs along a horizontal dual cycle (edges crossing a horizontal path in the dual) have been multiplied by $(-1)^i$ and along a vertical cycle have been multiplied by $(-1)^j$.

Now we have some way to calculate the partition function. We present the conclusions as follows.

Definition 3.2. Given any positive parameters z and w, we construct a *magnetically altered Kasteleyn matrix* $K(z,w)$ from K as follows: let γ_x and γ_y be horizontal and vertical paths. Multiply each edge crossed by γ_x by $z^{\pm 1}$ depending on whether the black vertex is on the left or the right, and similarly for γ_y.

For a double periodic graph G, we consider it's fundamental domain G_1, and let $P(z,w)=\det K(z,w)$ as the characteristic polynomial of G. Then $P\left((-1)^i,(-1)^j\right)=Z^{(ij)}$.

Theorem 3.3 ([8] Thm 3.3)**.** *Let P_n be the characteristic polynomial of G_n. Then*

$$P_n(z,w)=\prod_{z_0^n=z}\prod_{w_0^n=w}P(z_0,w_0).$$

Remark 3.2. *We give a scratch of the proof: based on the graph structure, we can find n^2 invariant subspace, and on each subspace, the determinant of K is a term in the product.*

Now, we have

$$\log P_n(z,w) = \sum_{z_0^n=z, w_0^n=w} \log P(z_0,w_0).$$

The right hand side can be view as a Riemann sum on the torus (for z_0 and w_0). After some effort, we can proof that the Riemann sum converge to the integral(This is not very easy, because there could be some pole on $\mathbb{T}^2$)

$$\frac{1}{n^2}\log Z_n^{(\theta\tau)} = \frac{1}{(2\pi i)^2}\iint_{\mathbb{T}^2} \log P(z,w)dzdw + o(1).$$

Theorem 3.4 ([8] Thm 3.5)**.** *Under the assumption that $P(z,w)$ has a finite number of zeros on the unit torus T^2, we have*

$$\log Z := \lim_{n\to\infty}\frac{1}{n^2}\log Z(G_n) = \frac{1}{(2\pi i)^2}\iint_{\mathbb{T}^2} \log P(z,w)dzdw$$

The quantity Z is the partition function per fundamental domain.

3.3 Link with a planar graph with slope

Here we use an example in [3] to give a direct interpolation. The general theorem can be found in [8] section 3.

As the setup in [3], we focus on the domino tilings, and we want to derive the entropy for a (boundary close to a square) region with tilt (s,t).

Now we introduce a weighted $2n \times 2n$ torus, with on each small square, the edge weight around the square is a, c, b, d in order, and satisfies $ac = bd$. We can find the link between the torus model and the tilt (s,t) planar model as follows:

1. It's difficult to directly derive a model with a given tilt (s,t) boundary. However, can use the torus to "create" a tilt (s,t) boundary, which is closed to the one we need.

2. For the weighted torus model we described before, conditional on a planar area, the configuration is *uniform*(as modified the edge pair a, b into c, d on a small square doesn't change the probability).

3. Combine 1 and 2, as we know that the number of outer boundaries is $\exp(o(n^2))$, we can express $ent(s,t)$ by the partition function in the torus.

Specifically, we have the following calculations:

Let $p_a := \mathbb{P}[a - edge]$ be the existence probability of a single "a-edge"(on torus all these probabilities equal), and that $p_a = N_a/2n^2$ (The number of "a-edge"). Where the latter can be expressed as $\mathbb{E}(N_a) = \frac{a}{Z_a}\frac{\partial Z_n}{\partial a}$ by definition.

When a, b, c, d distinct, we have $p_a \neq p_b$; while when we calculate the tilt, we use the number of $a - edge$ minus the number of $b - edge$ on the boundary to determine the slope change. Now if we can proof that all these existence probability are relatively "independent"(at least for large distance), then the typical boundary condition will converge to it's mean(In fact we can derive a large deviation result), i.e. with tilt $(s,t) = (2(p_a - p_b), 2(p_c - p_d))$. Hence with high probability, if we consider the outer planar boundary for each configuration, we know that (by Lemma 2.1 again) conditional on the boundary, the entropy inside is just the right we want.

Finally, as the number of outer boundaries are $\exp(o(n^2))$, we know that the entropy for tilt (s,t) equals:

$$\begin{aligned} ent(s,t) &= \lim \frac{1}{2n^2} \log Z_n(a,b,c,d) - \log\left(a^{\bar{N}_a} b^{\bar{N}_b} c^{\bar{N}_c} d^{\bar{N}_d}\right) \\ &= \log Z(a,b,c,d) - p_a \log(a) - p_b \log(b) - p_c \log(c) - p_d \log(d), \end{aligned}$$

where $Z_n(a,b,c,d)$ is the partition function on torus, and $\bar{N}_a$ donates the average number of a-edges in the torus.

Now, each term in RHS can be viewed as an integral on $\mathbb{T}^2$, we derive (after some calculations) the expected entropy expression.

3.4 The local limits

We have already known the limit shape of the configuration; then what we trying to understand is the fluctuations. Observing the hexagon and Aztec diamond as examples, we can see that the fluctuation behavior is quite different between the corner(frozen region) and the bulk(liquid region); it seems that this different behavior has a clear separation line. (called the *arctic curve*).

How to explain this phenomenon? We have a good interpolation via maximizing the entropy: in a typical configuration, the height function goes rapidly in the boundary, and minimal (maximal) at the corner. Therefore, in order to enable more configurations, the limit behavior should go up (down) with the maximum speed to a relatively "flat" region, and then go fluctuated.

In a word, the frozen phase can be explained as the region with an "extreme" slope in the limit shape.

3.4.1 link between weight and slope

In [8], the authors give a more general interpolation on the weighted double-periodic graph. The calculations are standard, while it introduces more interesting concepts in this field. In this report, we only give a scratch of the theory.

Let $\mu_{s,t}$ be the limit measure on $\mathbb{Z}^2$ be the limit measure of the measure on G_n with height change(ns, nt), we call it the Gibbs Measure of slope (s,t). (recall the free/wired Gibbs measure in the Ising model)

[9] proved that this family is the only possible translate invariant Ergodic Gibbs Measure(EGM). Let $\sigma(s,t)$ be the limit partition function per domain, called surface tension (or free energy), which correspond to $ent(s,t)$ in the previous section. We aim to invest the limit behavior of this measure.

Like the domino situation, we fixed all other weights in the fundamental domain, and left 2 degrees of freedom (B_x, B_y) in the weights, called the *magnetic flux* along a cycle winding once horizontally (resp. vertically) around the torus.

Then we calculate the (Weighted)partition function per fundamental domain(we call it *Ronkin function*) $F(B_x, B_y) := Z_{B_x,B_y}$. As the maximum slope can only be one (s,t) (which gives different slopes (s,t)) ([8]2.3.3), and that the weighted graph provides a term in the limit.

Hence we have: $F(B_x, B_y) = \max(-\sigma(s,t) + sB_x + tB_y)$, or

Theorem 3.5 ([8] Thm3.6)**.** *The surface tension $\sigma(s,t)$ is the Legendre transform of the Ronkin function of the characteristic polynomial P.*

3.4.2 Amoebae and 3 phases

Now we go to the main theory of this section. Recall that we can express F in a double periodic integral:

$$F(B_x, B_y) = \frac{1}{(2\pi i)^2} \iint_{T^2} \log P(e^{B_x} z, e^{B_y} w) \frac{dz}{z} \frac{dw}{w},$$

and for many other global terms, we can use the same method to give a double integral form. Specifically, we have the integral for the inverse Kasteleyn matrix K^{-1}, which is closely related to the covariance function. We have the following theorem.

Theorem 3.6 ([8]Thm 4.3)**.** *For the limiting Gibbs measure μ(with magnetic flux(0,0)), the probability of edges $e_1, ..., e_l$ exists in the configuration (where $e_j = (w_j, b_j)$), is*

$$\prod_j K(w_j, b_j) \det(K^{-1}(b_k, w_j))_{1 \le j,k \le l}$$

Moreover, assuming b and w are in a single fundamental domain, we have the following expression for K^{-1}:

$$K^{-1}(b, w + (x, y)) = \frac{1}{(2\pi i)^2} \iint_{T^2} K^{-1}(z, w) w^x z^y \frac{dz}{z} \frac{dw}{w} \tag{3.1}$$

Here $K^{-1}(z, w) = Q_{bw}(z, w)/P(z, w)$, where Q_{bw} is a polynomial in z and w.

The key observation is that: the asymptotic of the double integral totally depend on the behavior of the root $P(z, w) = 0$. If we consider the case with flux (B_x, B_y), then $P(z, w)$ will be replaced by $P(e^{B_x} z, e^{B_y} w)$, the behavior will depend on whether there's a root (z, w) in this polynomial.

This yield the famous *Amoebae*:

Definition 3.3 (Amoebae)**.** the amoeba $\mathbb{A}(P)$ of the polynomial $P(z, w)$ defined as the image of the curve $P(z, w) = 0$ in $\mathbb{C}^2$ under the map $(z, w) \to (\log|z|, \log|w|)$.

Based on the previous discussion, we observe that the typical behavior of K^{-1} inside/outside the amoebae (where $P(e^{B_x} z, e^{B_y} w)$ has/not has a root) is totally different. And that distinguishes the 3 phases as we want.

In fact, in [8] we have the following conclusions:

The flux (B_x, B_y) (with the correspond slope (s, t)) is in a:

Frozen phase. When (B_x, B_y) is in an unbounded component of the complement of the amoeba.

In these phases (s, t) lie on the boundary of the Newton Polygon(i.e. the set of all possible slopes).

Some of the height differences are deterministic— i.e., there exist distinct f and f' arbitrarily far apart for which $h(f)h(f')$ is deterministic.

liquid phase. When (B_x, B_y) is in the (open)interior of the amoeba, i.e. $P(e^{B_x} z, e^{B_y} w)$ either has two simple zeros on the unit torus or a real node on the unit torus.

In the case of simple zeros, $K^{-1}(b, w)$ decays linearly but not faster, as $|wb| \to \infty$. This implies that the edge covariances decay quadratically.

For the variance we have the following theorems:

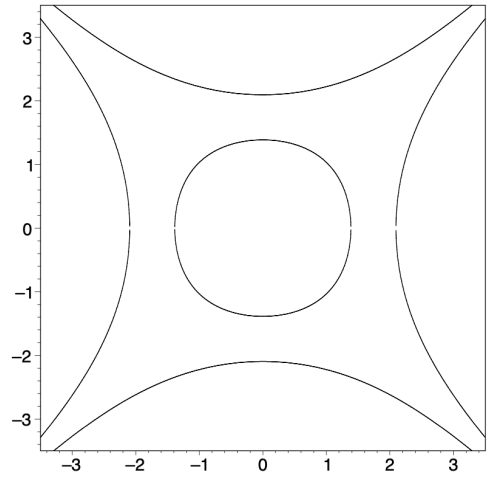

Figure 3.1: Amoebae for the polynomial $z + z^{-1} + w + w^{-1} = 6.25$, [8].

Theorem 3.7 ([8] Thm 4.5)**.** *Suppose that the zeros of P on T^2 are simple zeros at (z_0, w_0) and $(\bar{z}_0, \bar{w}_0)$. Let α, β be the derivatives of $P(z, w)$ with respect to z and w at (z0,w0). Then the height variance between two faces f_1 and f_2 is*

$$Var[h(f_1) - h(f_2)] = \frac{1}{\pi} \log |\phi(f_1) - \phi(f_2)| + o(\log |\phi(f_1) - \phi(f_2)|)$$

where ϕ is the linear mapping $\phi(x + iy) = x\alpha z_0 - y\beta w_0$.

Remark 3.3. *We can see that, in this case, the covariance behaves like a planar GFF.*

Gaseous phase. When (B_x, B_y) is in a bounded complementary component, $P(e^{-B_x} z, e^{-B_y} w)$ has no zeros on the unit torus.

As a consequence $K^{-1}(b, w)$ decays exponentially fast in $|b - w|$.

The height variance $h(f_1) - h(f_2)$ is bounded in the region.

Chapter 4

Converging to GFF

The main open problem in this field is the following conjecture:

Conjecture 1 (Kenyon-Okounkov)**.** *Consider the random tilings in domain R of size n. Then in the liquid region,*

$$h(nx, ny) - \mathbb{E}[h(nx, ny)] \to GFF,\ n \to \infty.$$

Where GFF is the Gaussian Free Field on L with respect to the complex structure given by ze^{-cy} with Dirichlet boundary conditions.

The GFF is normalized, so that

$$Cov(h(nx, ny), h(nx', ny')) \approx \ln d\big((x, y), (x', y')\big)$$

for $(x, y) \approx (x', y')$, with $d(\cdot, \cdot)$ denoting the distance in the local coordinates given by the complex structure.

Remark 4.1. *We should explain a little about this conjecture:*

There exists an analytic function $Q(v, w)$, such that the map $(x, y) \to (ze^{-cy}, (1 - z)e^{-cx})$ is a bijection of the liquid region L with (a part) of the curve $Q(v, w) = 0$ in $\mathbb{C}^2$, where $z(x, y)$ is chosen such that the slope $(h_x, h_y) = \frac{1}{\pi}(\arg z, \arg(1 - z))$

Remark 4.2. *A Gaussian free field in the region D can be defined as follows: GFF is a distribution such that for any test function u, v, $GFF_D(u), GFF_D(v)$ are mean 0 Gaussian random variables such that*

$$\mathbb{E}(GFF_D(u), GFF_D(v)) = \iint_{D\times D} u(z)G_D(z, z')v(z)dxdydx'dy'$$

Where G_D is the Green function in D. (boundary 0 and $\Delta G = \delta$)

Informally, we can view it as a random Gaussian function such that

$$\mathbb{E}(GFF_D(z)GFF_D(z')) = G_D(z, z') \sim \frac{-1}{2\pi} \ln|z - z'|,\ \textit{when } z \to z'$$

In this report, we first give the heuristics of the conjecture, then provide some approaches.

4.1 Heuristics

In [5] L12, we have a good heuristic for the Kenyon-Okounkov conjecture.

According to [3] we have

$$\mathbb{P}\left(h(nx,ny)/n \approx \tilde{h}(x,y)\right) \propto \exp n^2(\iint \sigma(\tilde{h}_x,\tilde{h}_y)dxdy + o(1))$$

In order to study the fluctuation around the limit shape h^*, let $\tilde{h} = h^* + \Delta h/n$. If we emit the error term $\exp(o(n^2))$, and after some calculations we have:

$$\mathbb{P}(\Delta h) \propto \exp(\pi i \int_L \frac{d\Delta h}{df}\frac{d\Delta h}{d\bar{f}})dfd\bar{f} + o(1),$$

which gives the right GFF fluctuations.

However, the large deviation results given in [3] is far from the right estimation. So we need other approaches.

Now recall that the n-edge correlation function can be expressed by the inverse Kasteleyn matrix $K^{-1}(x,y)$ (Thm 3.6), we only need to get an estimation on entries of K^{-1}. And now there are several approaches.

4.2 Approach: Counting the double integral

As we have the integral expression for K^{-1}, we have the asymptotic correlation function, and then the covariance of the height function. After writing the height correlations into integral form, we can use some analysis methods (steepest descent method, some approach via random matrix theory, differential operator, etc.) to deal with the convergence.

For more details see [5](Lecture 11, 14-25).

4.3 Approach: discrete holomorphic viewpoint in Temperley domain

Another viewpoint to deal with the inverse Kasteleyn matrix is to regard it as a discrete holomorphic function and then derives the convergence(via analysis or probability method). This section is mainly based on the classical paper of Kenyon [6], where one proofs the convergence in a special domain, called the *Temperley domain*.

For the symbols and pictures in this section, I refer to [10].

The key observation is as follows: consider the square grid with Kasteleyn matrix weight $i, -i, 1, -1$(in order). As we have $\sum_y K(x,y)K^{-1}(y,z) = \delta_{x,z}$, we get a relationship on $K^{-1}(\cdot,z)$, which can be viewed as a "discrete derivative operator".(see the definitions below) We have some standard argument that gives the convergence of discrete analytic function to real analytic one, provided that the boundary condition and poles correspond.

In a Temperley domain, we can naturally extend the boundary condition (of real or imagined part, respectively) to 0. A single pole is always existed and can be calculated out. Then by some analysis argument, we can prove the discrete function converges to a continuous analytic function, which is given by the Green's function, and we proved.

We now give explicit definitions.

Definition 4.1. Consider a domain on the plane $\mathbb{Z}^2$, and color vertex (x, y) by B_1, B_0, W_1, W_0 if $(x, y) \equiv (1, 0), (0, 1), (1, 1), (0, 0) \pmod{(2, 2)}$ respectively.

A Temperley domain is defined as follows: It is a polyomino where all convex corners are around a B_1 face and all concave corners are opposed to a B_1 face, with a single B_1 vertex at a corner removed(called the "root") to make the number of B and W equal.

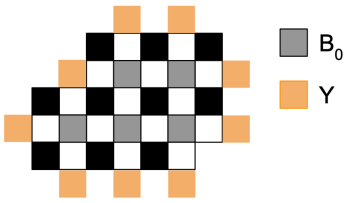

Figure 2.6: Temperley domain extension on the neighboring B_0 vertices Y

Figure 4.1: Temperley domain with extended boundary, [10].

Remark 4.3. *The Temperley domain is so chosen such that the boundary height is flat(so the limit shape is also flat, and only the liquid region remains).*

Definition 4.2 (discrete derivatives operator)**.** Let
$\partial_x f(v) = f(v+1) - f(v-1), \partial_y f(v) = f(v+i) - f(v-i)$,
$\partial_z = \partial_x - i\partial_y, \partial_{\bar{z}} = \partial_x + i\partial_y$
$\Delta = -\partial_z \partial_{\bar{z}}$.

Definition 4.3. A function F is discrete analytic on $\mathbb{Z}^2$ if it is *real* on $\mathbb{B}_0(\mathbb{Z}^2)$, *purely imagine* on $\mathbb{B}_1(\mathbb{Z}^2)$, null on $W(\mathbb{Z}^2)$, and if $\partial_{\bar{z}} F = 0$.

And we have the following Lemma:

Lemma 4.1. *The function $K^{-1}(v_1, v_2)$ satisfies:*
$K^{-1}(v_1, v_2) = 0$ *when v_1, v_2 both black or white.*
$K^{-1}(v_1, v_2) = K^{-1}(v_2, v_1)$.
For $v_1 \in W_0(P)$, $K^{-1}(v_1, v_2)$ is discrete analytic as a function of v_2 with a pole at v_1.

The most important observation is about the boundary condition as follows:

Lemma 4.2. *Consider the region P with Y its outer B_0 boundary.*
For $v_1 \in W_0(P)$ fixed, consider $K^{-1}(v_1, v_2)$ as a function of v_2 on $B_0(P)$. Then :
it is discrete harmonic on $B_0(P)/\{v_1 - 1, v_1 + 1\}$,
it extend to be 0 at the boundary on Y,
$\Delta Re K^{-1}(v_1, v_1 \pm 1) = \pm 1$.

Theorem 4.1. *For a fixed bounded region U, let $F_0(z_1, z_2)$ be an analytic function of z_2 with a simple pole of residue $1/\pi$ at z_1, and has real part 0 On the boundary of U.*
Then if v_1, v_2 is not too closed to the boundary, we have

$$\frac{1}{n} K^{-1}(v_1, v_2) = F_0(v_1, v_2) + o(1)$$

.

Now, after we have the convergence for K^{-1}, we can derive the n-point correlation of the height function, and then finishes the proof.

Theorem 4.2. *Let U be a bounded simply connected domain with smooth boundary in the plane. Let $a_1, \dots, a_k$ be distinct point in U, and $\gamma_1, \dots, \gamma_k$ are disjoint path running from the boundary of U to $a_1, \dots, a_k$.*

Let $h(z_i)$ denote the height of a point of P_ϵ lying with $O(\epsilon)$ of a_i, then as $\epsilon \to 0$, $\mathbb{E}(h^\epsilon - \bar{h}^\epsilon)(a_1) \cdots (h^\epsilon - \bar{h}^\epsilon)(a_k)$ converge to

$$\left| \sum_{\epsilon_1, \dots, \epsilon_k = \pm 1} \int_{\gamma_1} \cdots \int_{\gamma_k} \det_{i,j}(F_{\epsilon_i, \epsilon_j}(z_i, z_j)) dz_1^{(\epsilon_1)} \dots dz_k^{(\epsilon_k)} \right|$$

For a special kind of domain, (Temperley domain) the boundary condition of K^{-1} is just Dirichlet, so that we can prove that K^{-1} discrete harmonic converge to the solution of the (continuous) harmonic with Dirichlet BC(unique and can be determined for special domain)

However, in normal cases the boundary condition of K^{-1} is no longer Dirichlet, or even does not exists in continuous cases! In this situation, the behavior of K^{-1} is bad(the difference of K^{-1} can be large for a point that is close to each other so that no convergence result can be obtained)

(example: $K(a, b) = \sin a \sinh b$)

While although K^{-1} is not converged, the product of K^{-1} can converge. (like in the example)

4.4 Embedding, Aztec diamond, and minimal surface

Follows the idea in [6] and [7], recently [2] and [1] extend this method for some type of graphs. This approach is not complete up to now, while the "dream" is that it can be applied on all graphs and solve the Kenyon-Okounkov conjecture.

In this section, we only provide the vague idea, without a formal statement and proof. We refer to [1] for more details.

To introduce this approach, let us first look at the method in the previous section, and why it doesn't work for the Aztec diamond.

No valid limit function. In the Aztec diamond, we can also derive the discrete analytic property for K^{-1}. However, when dealing with the boundary condition, the case is different: in the Temperley domain, the outer "black" boundary is only of type B_1, so that we can naturally extend $K^{-1}(w, \cdot)$ to a function whose Imaginary part is 0. However, In the Aztec diamond, consider the top left edge, we can see that the boundary is of type both B_0 and B_1. That means that if we have the convergence, it should converge to a holomorphic function that is 0 on the boundary, which makes it vanish for the whole region!

The limit of K^{-1} not exists. Moreover, results have shown that when the shape is not flat, the inverse Kasteleyn matrix $K^{-1}(w_0, b)$ could behave "exp-badly" in distance, so that limit doesn't exist. In fact, it only exists in specific situations; and when it exists, is highly sensitive to the microscopic details of the boundary.

In all ways, we cannot directly use this approach for the Aztec diamond. The main problem is that we cannot deal with the problem with the frozen region. Recently, a new framework appears in solving this problem, that is the approaches by *embedding*.

4.4.1 Why embedding?

Recall the original proof, the key observation is that from $KK^{-1} = Id$, we choose properly the value K so that it gives a discrete analytic structure over K^{-1}.

However, the choice of K has some degree of freedom, that is:

For the absolute value $|K(w,b)|$, we can modify it into $\tilde{K}(w,b) = K(w,b)f(b)f(w)$, so that it doesn't change the probability measure: as the partition function multiply by $\prod_v f(v)$ for all configurations. (like the a, b, c, d weight in the previous section)

For the direction of K, the only thing we need is the alternative symbol around each 2k-face is $(-1)^{k+1}$.

In all, we can modify the weights $K(w,b)$ so that the *X-variable* of each face $b_1, w_1, \ldots, b_k, w_k$:

$$X_f = (-1)^{k+1} \prod_{i=1}^{k} \frac{K(w_i, b_i)}{K(w_i, b_{i+1})}$$

equals to the original weights, and the model doesn't change.

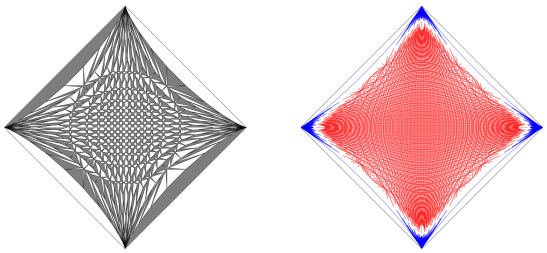

Figure 4.2: A perfect embedding for the Aztec diamond, [1].

Now, suppose that we have an embedding T: $G^* \to \mathbb{C}$ where G^* is the augmented dual (we can view it as the modification of the original "lattice graph", and each (inner) vertices correspond to a "face", so that for an edge (bw) and its dual edge u, v(direction: b on the left), we have $K(b,w) = T(u) - T(v)$ or $K(b,w) = dT(bw)$.

That is to say, it satisfies the *angle condition* (total black angle equals total white angle around a face) and the weight

$$X_f = (-1)^{k} \prod_{i=1}^{k} \frac{T(v) - T(v_{2i-1})}{T(v_{2i}) - T(v)}$$

From this, one can derive a conformal structure for the t-holomorphic function (but more complicated).

To proof the convergence, we introduce the so called *origami map* $O : G^* \to \mathbb{C}$, and then derive a closed form $PdT + QdO$ based on the conformal structure (we refer to [1] for details).

Now, consider the embedding $T + \alpha^2 O$ as a T-graph (see [7]). We only need to prove the convergence of discrete observables to the holomorphic functions in the metric of these embeddings.

Finally, we hope that when the embedding is "good", we can proof that the limit behavior $(T(x,y), O(x,y)) \to (z(x,y), \theta(x,y))$. Then based on the previous discussion we prove the convergence of the integral to the right correlation function.

In [1] one solved the problem when $\theta = 0$. We also mention that it is hopeful to prove the situation when z, θ forms a minimal surface (which corresponding to the Aztec diamond, see [2]). Here we give without proof the conclusion as follows.

Theorem 4.3 ([1]Thm1.4)**.** *Let t-embeddings T^δ approximate a bounded simply connected domain $\Omega \subset \mathbb{C}$. Assume that T^δ satisfy assumptions $Lip(\kappa, \delta)$ and $Exp-Fat(\delta)$ on compact subsets of Ω and*

(I) we are in the 'small origami' case: $O^\delta(z) \to \theta(z) = 0$ as $\delta \to 0$;

(II) the dimer model coupling function $K^{-1}(w^\delta, b^\delta)$ is uniformly bounded as $\delta \to 0$ provided that w^δ and b^δ remain at definite distance from the boundary of Ω and from each other;

(III) the correlations $H_n^\delta(v_1^\delta, ..., v_n^\delta)$ are uniformly small near the boundary of Ω:

$$H_n^\delta(v_1^\delta, ..., v_n^\delta) \to 0 \text{uniformly in } \delta \text{ as } dist(v_n^\delta, \partial\Omega) \to 0$$

provided that $v_\delta^1, ..., v_{n-1}^\delta$ remain at a definitive distance from each other and from $\partial\Omega$.

Then, the height function correlations $H_n^\delta(v_1^\delta, ..., v_n^\delta)$ converge to those of the GFF in Ω: for all $n \geq 2$ and all collections of pairwise distinct points $v_1, \ldots, v_n \in \Omega$, we have

$$H_n(v_1^\delta, ..., v_n^\delta) \to \pi^{-n/2} G_{\Omega_n}(v_1, \ldots, v_n) \text{ if } v_k^\delta \to v_k \text{ as } \delta \to 0.$$

Moreover, this convergence is uniformly provided that $v_1, \ldots, v_n$ remain at a definitive distance from each other and from the boundary of Ω.

However, there are still many questions unsolved in this setup: Is such embedding exists? Moreover, we need some regularity in the lattice, (Lip-κ, δ for $O(z)$, exp-fat(δ) for triangulation) to enable the convergence analysis in random walk; and that need more control for the embedding. So can we find a (series of) good enough embedding? And how to prove a given embedding is good? These questions are still open.

Chapter 5

Conclusion

We have solved the limit shape problem in [3], distinguished the 3 phases based on the inverse Kasteleyn matrix in [8].

For the fluctuation, i.e. the Kenyon-Okounkov conjecture, we have several approaches which lead to totally different directions.

One viewpoint is based on the Integrable probability: first writing down the covariance as the Riemann sum for a double integral; then proof the convergence (Riemann sum to the integral); finally, use analysis method to calculate the integral. (many conclusions are appeared in the notes [5]) However, this method is highly model-based and involves represent theory observations to write the covariance into a closed-form.

Another viewpoint is based on the conformal structure: one can write the inverse Kasteleyn matrix into a discrete harmonic function under a special structure (embedding). Then one can prove the convergence of discrete harmonic function to its harmonic limit. (refer to [6] [1] [2]) However, technical problems still remain in proofing the convergence and in finding a good enough embedding.

Both approaches can be applied to solve the conjecture for special models and domains. While solving the whole conjecture still remains a big open problem.

Bibliography

[1] Dmitry Chelkak, Benoît Laslier, and Marianna Russkikh. Dimer model and holomorphic functions on t-embeddings of planar graphs. *arXiv preprint arXiv:2001.11871*, 2020.

[2] Dmitry Chelkak and Sanjay Ramassamy. Fluctuations in the aztec diamonds via a lorentz-minimal surface. *arXiv preprint arXiv:2002.07540*, 2020.

[3] Henry Cohn, Richard Kenyon, and James Propp. A variational principle for domino tilings. *Journal of the American Mathematical Society*, 14(2):297–346, 2001.

[4] Béatrice de Tiliere. The dimer models in statistical mechanics. *Polycopie du cours*, 2014.

[5] Vadim Gorin. Lectures on random lozenge tilings. *Cambridge Studies in Advanced Mathematics. Cambridge University Press*, 2021.

[6] Richard Kenyon. Dominos and the gaussian free field. *Annals of probability*, pages 1128–1137, 2001.

[7] Richard Kenyon. Height fluctuations in the honeycomb dimer model. *Communications in Mathematical Physics*, 281(3):675–709, 2008.

[8] Richard Kenyon, Andrei Okounkov, and Scott Sheffield. Dimers and amoebae. *Annals of mathematics*, pages 1019–1056, 2006.

[9] Scott Sheffield. *Random surfaces: large deviations principles and gradient Gibbs measure classifications*. PhD thesis, Citeseer, 2003.

[10] Yijun Wan and Valentin Schmutz. Domino tilings and the gaussian free field. *Mémore de première année, ENS*, 2017.